RESILIENT INFRASTRUCTURE
June 1–4, 2016

NON-LINEAR FINITE ELEMENT ANALYSIS OF MODIFIED INFILLED STEEL AND CONCRETE FRAME SYSTEMS

Nabi Goudarzi
PhD Candidate in Structural Eng., University of Alberta, Canada

Mohammed Nazief
PhD Graduate of Structural Eng., University of Alberta, Canada

Yasser Korany
Former Associate Professor of Structural Eng., University of Alberta, Canada

ABSTRACT

To enhance the resiliency of framed structures under lateral loads, new infilled frame systems have been developed and evaluated using finite element method. The developed frame systems include haunches to reduce stress concentration at the frame's corners under lateral in-plane loads thus improving the resistance of the infilled frame system. A previously developed and validated three dimensional finite element models based on the simplified micro-modelling technique were adopted in this study to investigate the behaviour of infilled steel and reinforced concrete frames under lateral in-plane loads. The investigated parameters include: the infill wall stiffness, the presence and size of haunches at the beam-column connections. The effect of infill wall stiffness was investigated by analysis of steel and concrete frames infilled with grouted infill walls, which were found to significantly improve the lateral strength and stiffness of the infilled frames. The effect of the size of the haunches on the lateral behaviour of infilled frames was investigated by adding 200 mm, 400 mm, and 600 mm equal-leg haunches at the frame's beam-column connections. The lateral load resistance of infilled steel and reinforced concrete frames was found to increase by about 60% and 20%, respectively, when 600 mm equal-leg haunches were introduced. The Canadian standard for the design of masonry structures gave conservative estimates for the lateral cracking strength of the studied infilled frames. The accuracy of this standard was found to depend on the lateral stiffness of the bounding frames and the stiffness of the infill wall.

Keywords: Masonry infilled frames, haunched frames, steel frames, concrete frames, lateral strength, grouted masonry.

1. INTRODUCTION

In recent years, the concept of sustainability has expanded to include the requirement that structures be resilient. The requirements of longevity and the ability of structures to resist high lateral forces from the ever-increasing extreme natural events have become as equally important as the requirements of energy efficiency and low carbon emissions. In this paper, resilient lateral load resisting systems are defined as ones that have reduced probability of failure, reduced consequences from failures, and reduced time to rehabilitate. Resiliency is further defined as the ability to withstand loads without suffering significant degradation or loss of function (robustness), and capability to meet safety requirements in the event of degradation or loss of functionality (redundancy). Framed buildings lend themselves to the implementation of relatively simple measures to improve their resiliency to lateral forces.

Research has shown (Mehrabi et al. 1996, Dawe and Seah 1989) that the use of masonry infill walls tremendously increases the lateral load resistance of both steel and reinforced concrete frames. However, the response of infilled frames is much less ductile than bare frames. While in the past, clay brick infills were commonly used; concrete block infill walls are preferred in modern construction. Experimental studies by Liu and Soon (2012) demonstrated that fully grouted concrete block infill walls yield the highest contribution to lateral load resistance and the highest

increase in stiffness. However, infill walls are typically constructed after the completion of the frame skeleton and it is extremely difficult to grout a concrete block infill wall that has been constructed within an existing frame. Ungrouted (hollow) concrete block infill walls were found (Yanez et al. 2004, El-Dakhakhni et al. 2004) to lead to a sizable increase in lateral load resistance and stiffness but lower than fully grouted infills. In addition to the obvious difference in the effective cross sectional area, one of the main reasons for the lower contribution of hollow infills is their higher sensitivity to stress concentration at the corners of the surrounding frame.

The aim of this investigation is to develop and examine techniques to minimize the effects of stress concentration at the corners of steel and reinforced concrete frames on hollow concrete block infill walls. The proposed techniques include the introduction of beam haunches at frame corners. The objective of this investigation is to investigate the effectiveness of different size of beam haunches on the in-plane behaviour of concrete block infill wall in rigid reinforced concrete and flexible steel moment resisting frames.

2. REVIEW OF RELATED WORK

The in-plane response of masonry infilled steel and reinforced concrete has been the focus of many past and recent investigations. In an experimental investigation, Dawe and Seah (1989) studied the effect of several parameters on the behaviour of infilled frames using 28 full-size, single-bay steel frames infilled with 200 mm hollow concrete masonry units and type S mortar. Dawe and Seah reported that infill walls enhance the capacity of the containing frame even when there is a small gap between the infill and the frame or when the infill wall contains an opening. Tasnimi and Mohebkhah (2011) studied the performance of 5, two-third-scale steel frames infilled with solid clay brick units. It was reported that the presence of openings within the infill wall had no significant effect on the initial stiffness of the infilled frame.

Flanagan and Bennett (1999) studied eight full-size steel frames filled with hollow clay tile units. The infill wall thickness varied between a single wythe (195 mm thick) and a double wythe (330 mm thick). The size of the steel frame sections as well as the length and height of the infill wall varied to study the effect of frame stiffness on the infill wall behaviour. Flanagan and Bennett reported that all tested specimens failed through corner crushing, and surprisingly failure was relatively insensitive to the frame characteristics. Mehrabi et al. (1996) conducted a similar experimental investigation with 12 single-bay reinforced concrete frames infilled with concrete masonry and constructed at half-scale. Hollow and solid concrete masonry units were used to simulate weak and strong infills, respectively. Mehrabi et al. (1996) concluded that the presence of masonry infill wall within a concrete frame increases its capacity compared to bare frame and can be used to improve the performance of existing non-ductile concrete frames. Al-Chaar (1998) studied the performance of reinforced concrete frames infilled with concrete masonry units as well as clay brick units. The investigation was conducted on ½ scale specimens. The frames were single, double and triple bay with typical bay width of 2032 mm between centerlines of columns; the height of the infill walls was 1524 mm. It was found that the presence of stiffer masonry infill wall enabled the system to carry more load than the case of the bare frame. For multiple bay frames, the stiffness increased nonlinearly with the increase of the number of infilled bays. Most of the damage in the infill walls took place in the infill wall located near the loaded side.

In addition to experimental investigations, Finite Element Modelling (FEM) has also been used to evaluate the behaviour of masonry infilled structures. Dhanasekar and Page (1986) relied on nonlinear beam elements to model the frame and a nonlinear orthotropic model to represent the behaviour of brick infill panels. The interaction between the infill panel and the bounding frame was simulated using interface elements. Liauw and Lo (1988) modelled the frame and the interaction similarly, while the infill wall was modelled using a smeared cracking approach to simulate the effects of micro-cracking in the material. Stavridis and Shing (2010) developed a finite element model that combined the smeared and discrete cracking approaches to capture all possible failure mechanisms in the frame-infill system.

Smith and Carter (1969), Stafford-Smith and Coull (1991) and Mainstone (1971) used an equivalent strut approach to simulate the behaviour of masonry infill walls without openings, subjected to monotonic loading. A single strut was used to approximate the behaviour of the infill panel, reducing the analysis to that of a braced frame.
Despite the large number of investigations on the subject, no previous research was found where infilled haunched beam frames were investigated. To the best of the authors' knowledge, this investigation is the first to introduce and examine the effectiveness of this infill wall technique.

3. RESEARCH APPROACH

A nonlinear finite element modelling technique based on the simplified micro-modelling approach was adopted in this study. The technique has been developed by Nazief and Korany (2014) and validated against available experimental data and has been proven to be very effective in accurately predicting the entire lateral load–displacement behaviour of steel and reinforced concrete frames filled with masonry walls. To enable modelling the exact geometry of the masonry units, three-dimensional Finite Element Models (FEM) were constructed using the commercially available software, ABAQUS 6.10 (SIMULIA, 2010).

The three-dimensional 8-node solid element, C3D8R, was used to model reinforced concrete and steel frames and the masonry infill walls. This element has three translational degrees of freedom in the global directions for each node. Reduced integration scheme was used in analyzing the problem to reduce the computation time. The reinforcement for RC frames was modelled using the Beam Element, B31. This beam element has three translational and three rotational degrees of freedom at each node. The three-dimensional cohesive element, COH3D8, was used to model the interface between masonry units and that between the frame and the masonry infill wall.

For hollow concrete block, the masonry units were assigned material properties matching the compressive properties of hollow concrete block prisms. Analysis of the fully grouted masonry was simplified somewhat by modelling the units as solid blocks having the same properties as grouted masonry prisms. Material behaviour was defined by an elastic-plastic model for the steel and a concrete damaged plasticity model for the concrete and masonry. A more detailed description of the finite element modelling techniques employed is available in Nazief and Korany (2014).

Table 1: Material properties for the FEM models

Description	Value	Description	Value
Structural steel		Hollow concrete masonry blocks	
Yield strength (MPa)	350	Compressive strength	25
Ultimate strength (MPa)	450	Modulus of elasticity (GPa)	21.34
Modulus of elasticity (GPa)	200		
		Grouted concrete masonry blocks	
reinforcement		Compressive strength (MPa)	18
Yield strength (MPa)	400	Modulus of elasticity (GPa)	17.30
Modulus of elasticity (MPa)	200		
		Mortar	
Concrete frame		Shear strength (MPa)	1.2
Compressive strength (MPa)	30	Tensile strength (MPa)	0.1
Secant modulus of elasticity (GPa)	21.30		
Poisson ratio	0.25		

Structural steel was modelled using 350 MPa yield strength and 450 MPa ultimate strength. Steel reinforcing bars were assumed to have yield strength of 400 MPa. The value of the modulus of elasticity for steel was 200,000 MPa. The compressive strength and Poisson's ratio of the concrete for the RC frames was taken as 30 MPa and 0.25, respectively. The secant modulus of elasticity of concrete at 40% of the peak compressive strength was assumed to be 21,300 MPa. The compressive strengths of hollow and grouted concrete block infills were assumed to be 25 MPa and 18 MPa, respectively. The modulus of elasticity for hollow and grouted concrete block masonry were 21,336 MPa and 17,300 MPa, respectively. These values were measured by testing ungrouted and grouted concrete block assemblages constructed of the same block units and type S mortar (Nazief and Korany, 2014). The shear and tensile strengths of the mortar were assumed to be 1.2 MPa and 0.1 MPa, respectively, and the coefficient of friction between the masonry units was 0.7. Table 1 gives a summary of the material properties used in the numerical models. Loading was applied in the form of a quasi-static lateral displacement at the loading point of the masonry infilled frame. The corresponding lateral load was computed from the integration of the reactions at the frame base. Numerical analyses were conducted using the dynamic explicit solver in ABAQUS, which is suitable for analysis of structures with relatively short dynamic response time.

4. INVESTIGATED MODELS AND PARAMETERS

Finite element analyses were conducted on eight bare frames and eight infilled frames with hollow Concrete Masonry Units (CMU). The concrete masonry units consisted of 390 x 190 x 190 mm with void ratio of 47% and shell thickness of 32 mm. The frames included 2800 mm x 3600 mm (height x bay span) steel and concrete frames with and without haunches to investigate the effect of haunch on the lateral behavior of infilled frames. The haunches had equal leg sizes varying from 200 mm to 600 mm. Two analyses were also conducted on the infilled frames made of fully grouted CMU to study the effect of grouting on the lateral strength and stiffness of infilled frames. Table 2 shows the matrix and description of FEM analyses on bare and infilled frames. As shown in this table, SB and CB are steel and concrete bare frames without haunch, respectively. In Table 2, SB200 to SB600 and CB200 to CB600 are steel and concrete bare frames, respectively, where the numbers are the leg size of the haunches in mm. The SU and CU models are steel and concrete infilled frames without haunch, respectively; and, similarly, SU200 to SU600 and CU200 to CU600 are steel and concrete infilled frames with ungrouted CMU, respectively, where, again the numbers are the leg size of the haunches in mm. The two models SG and CG are inflled steel and concrete frames with grouted CMU.

Table 2: Analysis matrix of bare and infilled frames

Model designation		Frame beam configuration	Infill wall construction	Haunch leg size, e (mm)	Remarks
Steel	Concrete				
SB	CB	Flat	N/A	N/A	Bare frame, flat beam
SB200	CB200	Haunched	N/A	200	Bare frame, haunched
SB400	CB400	Haunched	N/A	400	Bare frame, haunched
SB600	CB600	Haunched	N/A	600	Bare frame, haunched
SU	CU	Flat	Ungrouted	N/A	Hollow CMU infill
SG	CG	Flat	Grouted	N/A	Grouted CMU infill
SU200	CU200	Haunched	Ungrouted	200	Haunched frame
SU400	CU400	Haunched	Ungrouted	400	Haunched frame
SU600	CU600	Haunched	Ungrouted	600	Haunched frame

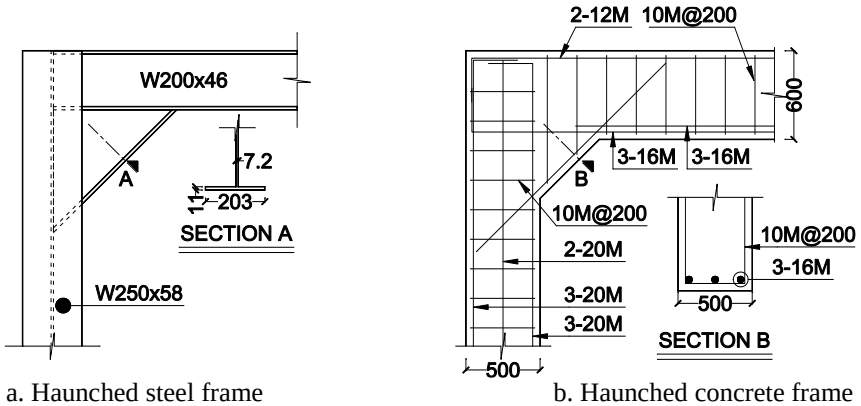

a. Haunched steel frame b. Haunched concrete frame

Figure 1: Details of the investigated a. steel, and b. reinforced concrete moment resisting frames.

Figure 1 shows the structural details of the concrete and steel frames. As shown in this figure the columns and the beam of the steel frame were W250x58 and W200x46, respectively. The bottom of the columns of the steel and concrete frames was fixed to a 5800 x 600 x 600 mm RC foundation. The steel beam was tied to the web of the column. The steel columns were oriented such that the strong axis was along the plane of the frame. The web and flange of the steel haunch were 7.2 mm and 11 mm thick, respectively. The concrete frames were modeled with 250 x 600 beam and 250 x 500 columns. The longitudinal reinforcement of the concrete columns included 20M bars and the stirrups included 10M bars spaced at 200 mm. The longitudinal bars of the concrete beam were 16M and 12M bars. The stirrups of the concrete beam were 10M spaced at 200 mm. The haunches in the concrete frames were reinforced with three 16M bars.

5. RESULTS AND DISCUSSION

Table 3 and 4 summarize the results for the modeled concrete and steel infilled frames. Figure 2 shows the principal compressive stresses for the investigated concrete and steel infilled frames without haunch at ultimate lateral load. This figure also illustrates diagonal tensile cracking (DT) along the compressive diagonal of the infill. As shown in this figure, a compressive strut formed in the infilled frames under lateral load. This figure shows that the compressive strut in the concrete infilled frame was wider than that in the steel infilled frame. Previous studies by Smith and Carter (1969) and Mainestone (1971) showed that as the lateral stiffness of infilled frames increases the compressive strut gets wider. The modeled concrete infilled frames were stiffer than the steel infilled frames, hence were expected to form a wider compressive strut than steel infilled frames. Figure 2 also shows that the principal compressive stresses vary throughout the compressive strut, showing concentration of compressive stresses at the corners of the infilled frames. These compressive stresses led to crushing of CMU at the corners of infilled frames, known as Corner Crushing (CC).

Table 3: Summary of the FEA results for the modeled infilled steel frames.

Frame designation	K_{bare} (kN/mm)	K (kN/mm)	P_{cr} (kN)	P_u (kN)	Δ_u (mm)	Failure mode
SU	2.4	127	340	424	17.3	CC[*1]
SG	2.4	347	577	975	18.7	DT[*2]+CC
SU200	3.2	147	339	491	20.0	CC
SU400	4.0	178	373	564	20.0	CC
SU600	4.8	189	375	677	20.0	CC

[*1] CC: Corner crushing, [*2] DT: Diagonal tension cracking.

Table 4: Summary of the FEA results for the modeled infilled concrete frames.

Frame designation	K_{bare} (kN/mm)	K (kN/mm)	$P_{cr}^{\dagger}$ (kN)	P_u (kN)	Δ_u (mm)	Failure mode
CU	32	294	450	611	17.3	CC[*]
CG	32	522	695	1070	9.3	DT[**]+CC
CU200	52	315	420	659	20.0	CC
CU400	58	420	560	726	20.0	CC
CU600	60	427	570	728	20.0	CC

[*] CC: Corner crushing, [**] DT: Diagonal tension cracking, $^{\dagger}P_{cr}$: load at first major crack.

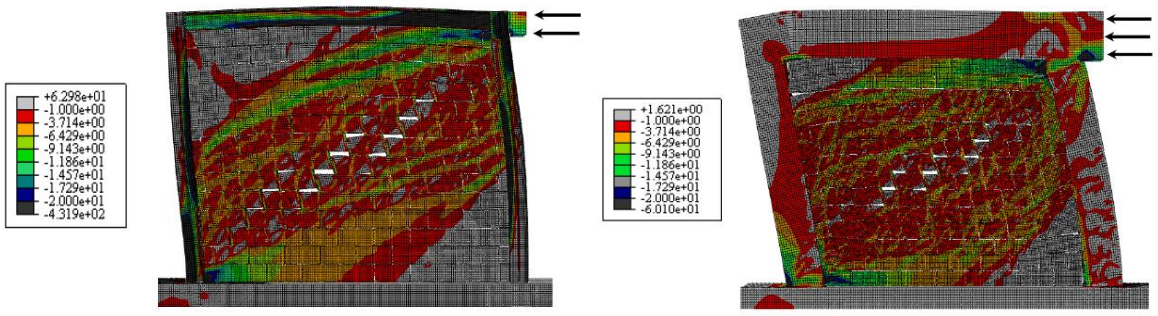

a. b.

Figure 2: Principal compressive stresses at ultimate load in a. steel infilled frames, and b. concrete infilled frames, with ungrouted CMU infills.

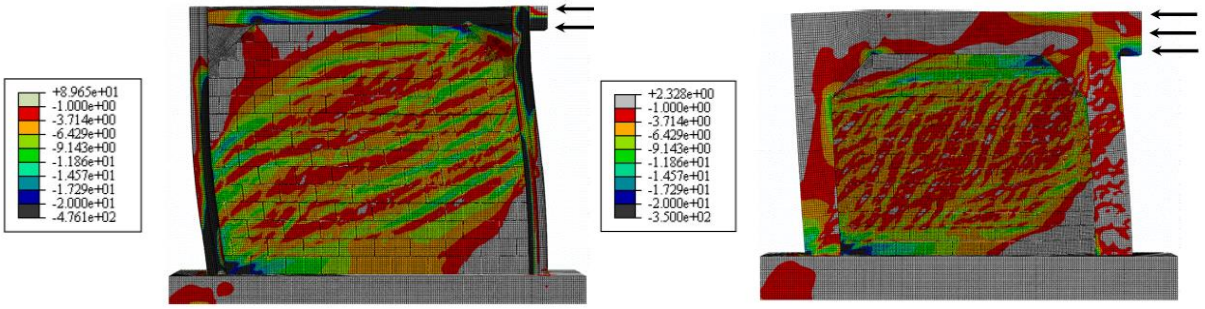

a. b.

Figure 3: Principal compressive stresses at ultimate load in huanched a. steel frames, and b. concrete frames infilled with hollow CMU walls.

Figure 3 shows the principal compressive stresses for the investigated concrete and steel infilled frames with haunches at ultimate lateral load. As shown in this figure, the compressive struts have become wider than those in the unhaunched infilled frames shown in Figure 2. Adding haunches to the infilled frames distributes the compressive stresses at the frame corners across a wider width of the compressive strut, thereby relieves the concentration of compressive stresses, and thus improves the lateral stiffness and ultimate lateral strength of infilled frames. Comparing Figure 2 with Figure 3 shows that the increase in the width of the compressive struts is more pronounced for the steel infilled frame than concrete infilled frames. Therefore, adding haunches is expected to make greater improvement to the ultimate lateral strength of the modeled steel infilled frames than concrete infilled frames.

Figure 4 shows the lateral load, P, against the lateral displacement, Δ, for the modeled bare and infilled frames. As expected, infilled frames had significantly higher lateral strength and stiffness than bare frames. As shown in Figure 4, the numerical lateral load of the investigated infilled frames increased almost linearly to an initial peak point, taken as the cracking strength P_{cr}, which is characterized by as sudden drop. After the post-cracking drop in lateral load resistance of the infilled frames, the lateral load increased again and exceeded the cracking strength of the infilled frames until it reached the ultimate lateral strength, P_u, at the ultimate lateral displacement, Δ_u. Figure 4 shows that the ultimate displacements of the steel and concrete infilled frames were about 20 mm, equal to a lateral drift (Δ_u/h) of 0.7% for the modeled infilled frames.

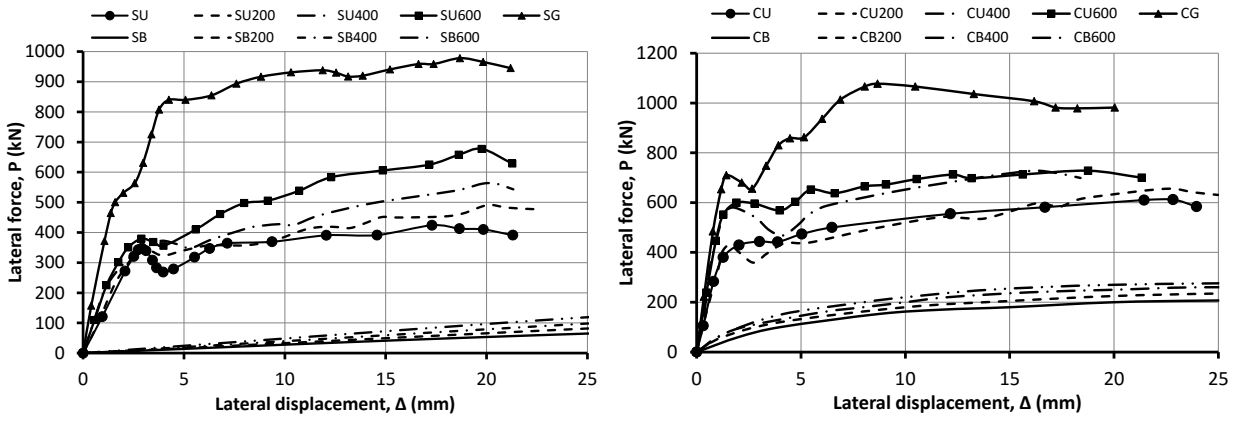

a. b.

Figure 4: Lateral load – displacement relationships for modeled a. steel and b. concrete bare and infilled frames.

Figure 4 shows that haunched infilled frames exhibit improved initial lateral stiffness, K, compared to unhaunched infilled frames. Part of this improvement is due to the improved stiffness of haunched bare frame with respect to unhaunched bare frame. For example Table 3 shows that the initial lateral stiffness, K, of the infilled frame SU600 is 62 kN/mm larger than the infilled frame SU, and the initial lateral stiffness of the bare frame, K_{bare}, of SU600 is 2.4 kN/mm larger than K_{bare} of SU. That is 3.9% (2.4/62) of the improvement in initial lateral stiffness of these infilled steel frames is due to the increased stiffness of the bare frame itself. Similar comparison between the initial

stiffness of the infilled concrete frames CU and CU600 and their respective bare frames show that 21% of the improvement in initial stiffness of these infilled concrete frames is due to the increased initial stiffness of the bare frame itself.

Figure 4 shows that introducing 400 mm and 600 mm equal-leg haunches in concrete infilled frames significantly improved their cracking strengths compared to concrete infilled frames without haunch and with 200 mm haunch. However, introducing haunches made negligible improvement to the cracking strength of the steel infilled frames. Figure 4-a. shows that for steel infilled frames, adding haunches improved post-cracking lateral stiffness of the steel infilled frame, which led to enhanced ultimate strength, P_u, in these infilled frames. However, introducing haunches did not improve post-cracking lateral stiffness of concrete infilled frames. Figure 4 also shows that infilled frames with fully-grouted infills exhibited significantly larger lateral strength and stiffness throughout loading than infilled frames with ungrouted CMU infills. In the numerical models, the failure mode for infilled frames with ungrouted CMU infills was corner crushing (CC), and for infilled frames with grouted CMU infills was Diagonal Tension cracking (DT) with corner crushing (CC).

Figure 5 shows the lateral stiffness ratio K_r against the leg size of the haunch, e, for the steel and concrete infilled frames. The stiffness ratio is defined as K/K_{SU} and K/K_{CU} for steel and concrete infilled frames, respectively, where K_{SU} and K_{CU} are the initial stiffness values of unhaunched steel and concrete frames infilled with hollow CMU, respectively. As shown in Figure 5, the lateral stiffness ratio for the investigated steel and concrete infilled frames increased almost linearly up to nearly 1.5 as the haunch leg-size increased from 200 mm to 600 mm.

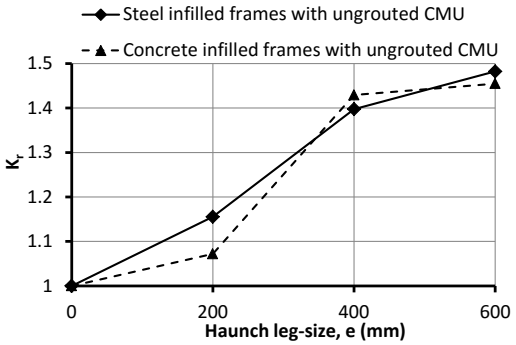

Figure 5: Stiffness ratio against haunch leg-size for steel and concrete infilled frames with ungrouted CMU.

Figure 6 shows the cracking and ultimate strength ratios - $P_{cr,r}$ and $P_{cr,r}$, respectively - against the haunch leg-size, e, for the investigated steel and concrete infilled frames. The cracking strength ratio is defined as $P_{cr}/P_{cr,SU}$ and $P_{cr}/P_{cr,CU}$ for the investigated steel and concrete infilled frames, respectively, where $P_{cr,SU}$ and $P_{cr,CU}$ are the cracking strengths of the unhaunched steel and concrete infilled frames, respectively. Similarly, the ultimate strength ratio $P_{u,r}$ is defined as $P_u/P_{u,SU}$ and $P_u/P_{u,CU}$ for the investigated steel and concrete infilled frames, respectively, where $P_{u,SU}$ and $P_{u,CU}$ are the ultimate strengths of the unhaunched steel and concrete infilled frames, respectively. Figure 6.a. shows that the cracking strength ratio was improved up to 10% for steel frames and 28% for concrete infilled frames when 600 mm equal-leg haunches were introduced to the frames. Figure 6.b. shows that the ultimate strength ratio was improved up to 60% for steel infilled frames and only up to 20% for the concrete infilled frames when 600 mm equal-leg haunches were introduced to the frames. In other words, adding haunches made more improvement to the ultimate lateral strength of steel infilled frames than concrete infilled frames. This can be attributed to the higher impact of adding haunches on the compressive struts of the steel infilled frames, than concrete infilled frames. The concrete infilled frames did not benefit from haunches as much as the steel infilled frames, since concrete infilled frames were already stiff enough to form wide compressive struts.

Moreover, Figure 6 shows that the effect of haunches on the ultimate lateral strength is larger than on the cracking strength of the infill. This could be expected since the diagonal cracking of the infill corresponds to the shear and tensile failure of the mortar joints of the infill and tensile cracking of the masonry units, but the ultimate lateral strength of the infill corresponds to the crushing of the masonry units at the corners of the infill. And haunches reduce the stress concentration at the corners, and thus improve the ultimate lateral strength of the infilled frame.

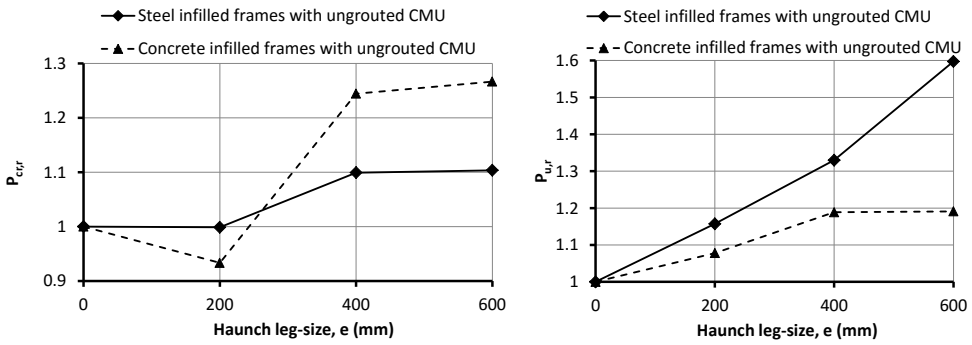

a. b.

Figure 6: Ratio of a. cracking, and b. ultimate strengths against haunch leg-size for steel and concrete infilled frames

As shown by this analytical study introducing haunches improves the initial stiffness and ultimate strength of infilled steel and concrete frames. Improved stiffness of huanched infilled frames increases the lateral seismic forces on the building, which in turn exerts larger lateral forces on the infilled frames. Therefore, when this infilled frame system is used in designing or retrofitting of buildings, the combined effect of increase in stiffness and strength of the building should be considered.

6. ANALYTICAL STUDY USING CAN/CSA S304-14

The numerical cracking strength and ultimate lateral strength of the investigated infilled frames are compared with the estimated values given by the Canadian code for design of masonry structures (CAN/CSA S304-14). The estimated cracking strength, V_c, is given by Equation 1 as per CAN/CSA S304-14.

[1] $$V_c = \phi_m (v_m b_w d_v + 0.25 P_d) \gamma_g$$

Where, ϕ_m is the strength reduction factor taken as 1.0 in this study, v_m is the shear strength of the masonry, b_w is the thickness of the wall and d_v is the effective depth for shear calculations taken as the length of the wall. In equation 1, P_d is the dead load, which is taken as zero in this investigation since dead load was not applied in the numerical models. Also, γ_g is a correction factor to account for the amount of grouting. In this investigation, γ_g is taken as 1.0 and b_w for ungrouted infills is taken as twice the shell thickness of CMU, i.e. 2 x 32 mm, and for grouted infills is taken as the entire thickness of infill, 190 mm. The shear strength v_m for ungrouted infills is taken as the shear strength of the mortar in the numerical models, 1.2 MPa. And v_m for grouted infills is taken as the minimum value prescribed by CAN/CSA S304-14, which is $0.16\, f_m^{0.5}$, where f_m is the compressive strength of the masonry prism normal to the bed joints.

To calculate the ultimate strength of infilled frames, the infill is assumed as a compressive strut with width and thickness equal to w_e and t_e, respectively. The width of the compressive strut is given by CAN/CSA S304-14 and is limited to one quarter of the diagonal length of the infill. For ungrouted infills, t_e is taken as twice the shell thickness CMU and for grouted infills t_e is taken as the entire thickness of the infill, 190 mm. The compressive strength of this strut, F, is given by Equation 2 as per CAN/CSA S304.1-14.

[2] $$F = 0.85 \phi_m \chi f_m w_e t_e$$

Where, ϕ_m is the strength reduction factor taken as 1.0, χ is the directionality factor of masonry compressive strength taken as 0.5 here to conservatively assume the compressive stresses are parallel to the bed joints. The estimated ultimate lateral strength of the infilled frames, V_u, is assumed to be provided only by the diagonal compressive strut. Hence, the ultimate lateral strength can be found by Equation 3.

[3] $$V_u = F\cos(\theta) = F/\sqrt{1 + (h/l)^2}$$

Where θ is the angle of the diagonal strut with the horizontal, h and l are the height and length of the infill wall, respectively. Table 5 compares the numerical results with the predicted results using CAN/CSA S304-14. Table 5 shows that P_{cr}/V_{cr} varies between 1.23 to 1.36 for steel infilled frames and between 1.49 to 2.07 for concrete infilled frame. This means CAN/CSA S304-14 gives conservative estimates for the cracking strength of the infilled frame. This table also shows that P_u/V_u for unhaunched steel and concrete infilled frames are 0.84 and 1.0, respectively. This shows that for concrete infilled frames where the members possess large flexural stiffness, the estimated ultimate lateral strength, V_u, estimated by CAN/CSA S304-14 is close to the numerical results. However, for steel infilled frame with small flexural stiffness, Equation 3 overestimates the ultimate lateral strength of the infilled frame. For steel and concrete infilled frames with grouted CMU infills, P_u/V_u is 0.88 and 0.82, respectively, which means Equation 3 overestimates the ultimate lateral strength of the investigated infilled frames with grouted infills. Therefore, it can be concluded that when the lateral stiffness of the infill to the lateral stiffness of the bounding frame is large CAN/CSA S304-14 overestimates the ultimate lateral strength of the infilled frame.

Table 5: Comparison of numerical results with estimated results using CAN/CSA S304-14

Investigated model	V_{cr} (kN)	P_{cr}/V_{cr}	w_e/D	V_u (kN)	P_u/V_u
Steel Infilled frames					
SU	276	1.23	0.206	505	0.84
SG	465	1.24	0.166	1107	0.88
SU200	276	1.23	0.206	505	0.97
SU400	276	1.35	0.206	505	1.12
SU600	276	1.36	0.206	505	1.34
Concrete infilled frames					
CU	276	1.63	0.250	611	1.00
CG	465	1.49	0.250	1307	0.82
CU200	276	1.52	0.250	611	1.08
CU400	276	2.03	0.250	611	1.19
CU600	276	2.07	0.250	611	1.19

As shown in Table 5 for steel infilled frames, the calculated width of the compressive strut is less than maximum width of diagonal strut specified by CAN/CSA S304.1-14, i.e. one quarter of the diagonal length of the infill. In this case, adding haunches increases the width of the compressive strut, and thus improves the ultimate lateral strength of the infill. Hence, the ultimate lateral strength was improved by 60% when 600 mm equal-leg haunches were added to the infilled frames. However, for the concrete infilled frames, the compressive strut had the maximum width allowed by CAN/CSA S304-14. Therefore, adding haunches did not increase the design width of the compressive strut, which is consistent with the numerical results shown in Figure 3. Hence, adding haunches to concrete infilled frames is expected to improve the ultimate lateral strength to a lesser extent than adding haunches to steel infilled frames. This can explain why adding 600 mm haunches only made 19% improvement of ultimate lateral strength of concrete infilled frames (Table 5) compared to 60% improvement in the case of steel infilled frames.

7. CONCLUSIONS AND RECOMMENDATIONS

Finite element analyses were conducted on steel and concrete infilled frames to investigate the effect of haunched frames and grouted infills on the lateral strength and stiffness of infilled frames. The numerical results were also compared with the lateral strength and stiffness estimated by the Canadian standard for the design of masonry structures.

It was found that infilled frames with grouted infills exhibit larger lateral cracking and ultimate strengths, and lateral stiffness than infilled frames with hollow infills. Adding haunches significantly improved the ultimate lateral strength of the studied infilled frames, depending on the lateral stiffness of the bounding frame. For steel infilled frames, where the bounding frame had low stiffness, adding haunches improved the ultimate lateral strength up to 60%. Adding haunches also improved the cracking lateral strength and lateral stiffness of the studied infilled frames, but it was not as significant as the improvement in the ultimate lateral strength.

CAN/CSA S304-14 yields conservative estimates for the cracking lateral strength of infilled frames by up to 100%. Estimates from CAN/CSA S304-14 were in good agreement with the numerical ultimate lateral strength of the studied unhaunched concrete infilled frame, but overestimated the lateral strength of unhaunched steel infilled frame with hollow infill by 16%. The Canadian standard for the design of masonry structures was found to overestimate the lateral ultimate strength of the studied infilled frames with grouted infills.

ACKNOWLEDGEMENTS

Funding for the investigation reported in this paper was provided by the Natural Sciences and Engineering Research Council of Canada.

REFERENCES

Al-Chaar, G. 1998. *Non-Ductile Behaviour of Reinforced Concrete Frames with Masonry Infill Panels Subjected to In-Plane Loading*, PhD thesis, University of Illinois, Chicago, Illinois, USA.

CAN/CSA S304-14. 2014. *Design of masonry Structures.* Canadian Standards Association, 5060 Spectrum Way, Suite 100, Mississauga, ON, Canada.

Dawe, J. L., and Seah, C. K. 1989. Behaviour of masonry infilled steel frames. *Canadian Journal of Civil Engineering*, 16(6), 865-876.

Dhanasekar, M., and Page, A. W. 1986. The influence of brick masonry infill properties on the behavior of infilled frames. *Proceedings of the Institution of Civil Engineers – Engineering History and Heritage*, 139, 170-181.

El-Dakhakhni, W., Hamid, A. A., and Elgaaly, M. 2004. Seismic retrofit of concrete-masonry-infilled steel frames with glass fiber-reinforced polymer laminates. *Journal of .Structural Engineering*, 130(9), 1343-1352.

Flanagan, R. D., and Bennett, R. M. 1999. In-plane behavior of structural clay tile infilled frames. *Journal of Structural Engineering*, 125(6), 590-599.

Liauw, T.C., and Lo, C.Q. 1988. Multibay infilled frames without shear connectors. *ACI Structural Journal,* July-Aug, 423-428.

Liu, Y., Soon, S. 2012. Experimental study of concrete masonry infills bounded by steel frames. *Canadian Journal of Civil Engineering*, 39(2), 180-190.

Mainstone, R. J. 1971. On the stiffnesses and strengths of infilled frames. *Proceedings of the Institution of Civil Engineers, Proceedings,* 4, 57-90.

Mehrabi, A. B., Shing, P. B., Schuller, M. P., and Noland, J. L. 1996. Experimental evaluation of masonry-infilled RC frames. Journal of Structural Engineering, 122(3), 228-237.

Nazief, M. and Korany, Y. 2014. Finite Element Modelling Technique for Masonry Infilled Shear Walls with and without Openings. *4th Annual International Conference on Civil Engineering*, The Athens Institute for Education and Research, Athens, Attica, Greece, 12 p.

SIMULIA, 2010. *ABAQUS 6.10 EF-2 Theory Manual,* Abaqus, Providence, Rhode Island, USA.

Smith, B. S., and Carter, C. 1969. A Method of Analysis for Infilled Frames. *Proceedings of the Institution of Civil Engineers*, 44, 31-48.

Stafford-Smith, B., and Coull, H. 1991. Chapter 8: Infilled-Frame Structures. *Tall Building Structures: Analysis and Design*, John Wiley and sons. Inc., New York, USA, 168-183.

Stavridis, A., and Shing, P. B. 2010. Finite-element modelling of nonlinear behavior of masonry-infilled RC frames. *Journal of Structural Engineering*, 136(3), 285-296.

Tasnimi, A. A., and Mohebkhah, A. 2011. Investigation on the behavior of brick-infilled steel frames with openings, experimental and analytical approaches. *Engineering Structures*, 33(3), 968-980.

Yàñez, F., Astroza, M., Holmberg, A. and Ogaz, O. 2004. Behavior of confined masonry shear walls with large openings. *Proceedings of the 13th world conference on Earthquake engineering*, Vancouver, B.C., Canada, 14 p.